Beyond photon pairs

Yorulmaz, S.Ç.

CHAPTER 2

Characterization of pulsed parametric down-conversion in PPKTP crystals

We experimentally characterize sources of frequency degenerate down-converted photons at 826.4 nm generated in 2 mm, 5 mm and 10 mm long periodically-poled KTP crystals. The crystals are pumped by 413.2 nm laser pulses with 2 ps duration. The dispersion D=1.5 ps/mm puts a limit to the length over which phase matching is efficient for a 2 ps pulse and provides a lower limit for the angular width of SPDC in the far-field. We investigate the far-field distribution of SPDC produced by periodically-poled KTP crystals and compare this with the calculated intensity distribution and find good agreement with theory. We also discuss the performance of PPKTP in terms of nonlinearity and group velocity walk-off compared to other available materials.

S. Cigdem Yorulmaz and Michiel J.A. de Dood, *Characterization of parametric down-conversion in periodically poled KTP crystals with a picosecond pump*, Proc. SPIE 8440, 84400G (2012).

2.1 Introduction

Spontaneous parametric down-conversion (SPDC) is a second order nonlinear process that converts a high energy pump photon into two highly correlated signal and idler photons at lower energy. Because of the strong correlations between the photons, SPDC is a good candidate for creating entangled photons. Sources of polarization [1, 2], frequency [3, 4], time-bin [5, 6] and spatially [7–9] entangled photons all have been demonstrated.

Here we consider spatially entangled photons with the same polarization, which can be described by the transverse photon momentum. Generating such spatially entangled single photon pairs has been demonstrated using continuous wave lasers as a pump. However, in order to create spatially entangled multi-photon states, the photons should be generated within a coherence time of the photon pairs set by either a bandpass filter or the intrinsic width of the down-conversion. Since these coherence times are typically in the 10-1000 fs range, the use of short laser pulses is a requirement to observe multi-photon events.

In this Chapter, we present an experimental characterization of SPDC sources created using periodically-poled KTP (PPKTP) crystals with different length pumped by a picosecond pulsed laser. We discuss the effect of group velocity walk-off in PPKTP using the group velocity mismatch. To compare the characteristics of the pulsed SPDC source, we compare our results to the calculated intensity distribution of a continuous wave pumped SPDC source based on PPKTP. We also discuss the efficiency for pulsed SPDC of different crystal types such as PPLN, BBO, LBO and $LiIO_3$ compared to PPKTP crystal.

2.2 Phase matching in pulsed down-conversion

In a parametric down-conversion process, energy is conserved, and therefore the frequencies of the photons are related via $\omega_p = \omega_s + \omega_i$ where p, s and i correspond to pump, signal and idler photons, respectively. For an efficient process, photons are expected to satisfy the phase matching condition $\mathbf{k_p} = \mathbf{k_s} + \mathbf{k_i}$, where $\mathbf{k_p}, \mathbf{k_s}, \mathbf{k_i}$ represent the wavevector of the pump, signal and idler photons. Here we consider a frequency-degenerate type-I SPDC process in a PPKTP crystal, where pump, signal and idler photons have the same polarization, while signal and idler photons have the same frequency

($\omega_p = 2\omega_s = 2\omega_i$). To simplify the notation, we use $k_{2\omega}$ and k_ω for the wavenumber of the pump and SPDC photons.

Phase matching of down-conversion generated by continuous-wave (cw) pumping is well known and has been extensively described for PPKTP crystals [10]. For a pump beam polarized in the z-direction and propagating in the x-direction of the crystal, the transverse wavevector mismatch in the $y-z$ plane is approximately zero i.e. ($q_s \approx -q_i$), while the longitudinal wavevector mismatch is non-zero due to the temperature-dependence of the refractive index of the PPKTP crystal. Hence, the temperature of the PPKTP crystal determines the geometry of the SPDC light in the $y-z$ plane, and the far-field intensity distribution can be either an open ring shape (non-collinear) or a disk shape (collinear).

The far-field intensity distribution of SPDC light generated by a plane-wave, cw pump beam can be written as [10]

$$I(q,T) \propto \mathrm{sinc}^2\left(\frac{L}{2k_\omega}q_\omega^2 + \varphi(T)\right) \tag{2.1}$$

where q_ω and k_ω are the transverse momentum and wavenumber of the down-converted photon, L is the crystal length and $\varphi(T)$ is a temperature-dependent longitudinal phase mismatch. Collinear SPDC corresponds to $\varphi(T) = 0$ and occurs only for a specific crystal temperature.

We consider frequency-degenerate down-conversion generated by picosecond laser pulses in the same PPKTP crystal. Since a pulsed pump has a nonzero spectral width, the phase matching condition should be modified to contain the effect of this spectral width of the pump. We use a first order Taylor expansion of the wavevector mismatch for frequency-degenerate SPDC to include the effect of dispersion on the phase matching condition [11]

$$\Delta k(\Omega) \approx (k_{2\omega} - 2k_\omega) + D\Omega. \tag{2.2}$$

Here D is the dispersion that contains the group velocity mismatch between pump and down-converted photons and is defined as $D = 1/v_g(2\omega) - 1/v_g(\omega) = (n_g(2\omega) - n_g(\omega))/c$ with v_g and n_g the group velocity and group index. The frequency Ω is the detuning of the pump frequency relative to the center frequency of the pump. Note that to arrive at Eq. (2.2), we have used the fact that pump and down-converted photons all have the same polarization [11], and that we neglect the relatively small phase-mismatch due to differences in the frequency of the SPDC

photons. This second simplification corresponds to a typical experimental situation where the SPDC light is filtered by a narrow bandpass filter with a bandwidth much smaller than the natural bandwidth of the source. For comparison, the natural phase matching bandwidth for a 2 mm PPKTP crystal is around 40 nm, while the bandpass filter has a FWHM width of 1 nm, which selects SPDC light close to frequency degeneracy. For the UV pulsed pump (λ=413.2 nm) used in the experiment, the difference in group index is $n_g(2\omega) - n_g(\omega) = 0.4564$ for the PPKTP crystal at a temperature of 300 K and the corresponding group velocity dispersion D = 1.5 ps/mm [12]. In the calculation, we assume a plane-wave pump beam with a Gaussian envelope function to represent the frequency content of the pulsed pump. The intensity distribution for pulsed down-converted photons generated in PPKTP can then be written as

$$I(q,T) \propto \frac{1}{\sigma\sqrt{2\pi}} \int_{\Omega} d\Omega \exp\left(-\frac{1}{2}(\Omega/\sigma)^2\right) \times \operatorname{sinc}^2\left(\frac{L}{2k_\omega} q_\omega^2 + \varphi(T) + \frac{1}{2} D\Omega L\right) \tag{2.3}$$

where σ is defined as the standard deviation of the intensity distribution in the angular-frequency domain and τ_p is the duration of the pulse defined at FWHM [13]. The corresponding time-bandwidth product for a transform-limited gaussian pulse is defined by $\sigma\tau_p \approx 1.18$. For efficient conversion of all spectral components in the pulse, the condition of $DL < \tau_p$ has to be satisfied. Thus, the group velocity walk-off length $L_w = \tau_p / D$ is a typical length over which the SPDC process is efficient. For crystals longer than this walk-off length, the pulse duration of the SPDC light is significantly broadened compared to the pump pulse [14].

In order to visualize the role of group velocity walk-off in the pulsed down-conversion process, we calculate the angular width of the collinear SPDC light as a function of crystal length for both cw (Eq. 2.1) and pulsed laser pump (Eq. 2.3). The calculation is performed assuming a transform-limited gaussian pulse with 2 ps duration, which has an angular frequency bandwidth $\sigma = 0.59$ rad/ps. Fig.2.1 shows the calculated width (FWHM) of the far-field intensity distribution for collinear SPDC for continuous-wave (red solid line) and a pulsed pump (black solid line) as a function of crystal length on a log-log scale. The inset of Fig.2.1 shows the calculated angular intensity distribution of SPDC light for cw pumping (red solid line) and

for pulsed pumping (black solid line) considering a group velocity walk-off length $L_w = 1.3$ mm. At this length, the pulsed nature of the pump removes the distinct local minima of the sinc function while the width of the peak is comparable. As can be seen in Fig.2.1 for cw pumping, the angular width decreases inversely proportional to $\sqrt{L}$ while the angular width of pulsed SPDC light starts saturating when the crystal is longer than walk-off length L_w. For short crystals ($L \lesssim 0.3$ mm), the effect of dispersion can be ignored and the phase matching conditions for cw and pulsed SPDC become identical.

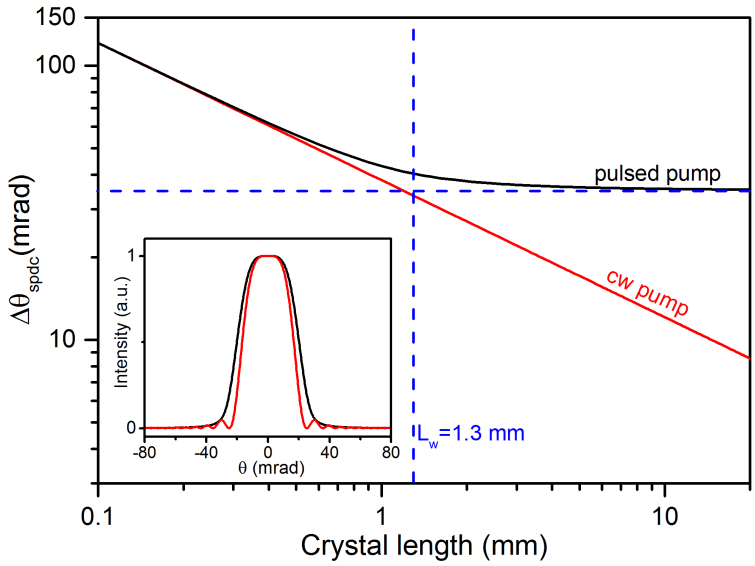

Figure 2.1: Calculation of the angular width (FWHM) of collinear ($\varphi = 0$) down-converted light as a function of crystal length for both cw (red solid line) and pulsed (black solid line) SPDC process. The pulsed pump is assumed to be a transform limited gaussian pulse with a spectral width $\sigma = 0.59$ rad/ps for a 2 ps pulse. The horizontal dashed line indicates the limit of angular width where the width saturates for a pulsed pump. This occurs for crystal lengths longer than the walk-off length of 1.3 mm (vertical dashed line). The inset shows the calculated normalized intensity versus angle of collinear SPDC light generated by cw (red solid line) and pulsed (black solid line) laser for a crystal length of 1.3 mm.

2.3 Experimental characterization of a pulsed SPDC source

In our experiment, we use periodically-poled KTP crystals (potassium titanyl phosphate (KTiOPO4)) designed for type-I phase matching by temperature tuning of the crystal. The crystals of various lengths are pumped by a weakly focussed (w_p =100 μm) linearly polarized pulsed laser propagating along the x-axis of the crystal. The length of the crystals are 2 mm, 5 mm and 10 mm in the x-direction and all crystals have a width of 2 mm and a height of 1 mm. The poling period of the PPKTP crystal $\Lambda_0 = 3.675$ μm is designed to enable collinear phase matching at a crystal temperature of 50°C to generate vertically polarized SPDC light at the frequency degenerate wavelength of 826.4 nm.

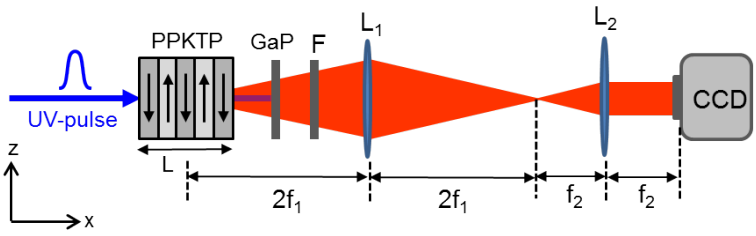

Figure 2.2: Schematic of the experimental setup to record far-field images of down-converted light. A periodically poled KTP crystal is pumped by 413.2 nm frequency-doubled Ti:Sapphire laser producing 2 ps pulses at a repetition rate of 80 MHz. The pump light is removed from down-converted light using anti-reflection coated GaP wafer. A bandpass filter F centered around 826.4 nm with a bandwidth of 1 nm is used to collect frequency degenerate SPDC light. The lenses L_1 ($f_1 = 50$ mm) and L_2 ($f_2 = 25$ mm) create a far-field image that is recorded by a CCD camera.

Figure 2.2 illustrates the experimental setup to obtain far-field images of the generated SPDC light. UV pulses at a wavelength of 413.2 nm with a duration of $\tau_p \approx 2$ ps are produced by frequency-doubling a Ti:Sapphire laser are focussed into a PPKTP crystal to create frequency degenerate down-converted photons at 826.4 nm. The average power of the UV pulses is kept constant at 170 mW. A GaP wafer that is anti-reflection coated for 826 nm is used to block the residual pump light in the experiment. In order to detect only frequency degenerate photons ($\omega_s \simeq \omega_i$), we use a narrow bandpass filter centered at 826.4 nm with a bandwidth of 1 nm which is much

narrower than phase-matching bandwidth of SPDC light (40 nm for a 2 mm PPKTP crystal). The two lenses with focal distances of 50 mm and 25 mm are used to create a far-field image of the down-converted light on the CCD camera. The temperature of the PPKTP crystal is controlled via a Peltier element with a PID controller, which keeps the temperature constant within 10 mK. Temperature-dependent far-field images of the SPDC source are recorded by a CCD camera for the temperature range of 10-50°C.

The temperature dependence of the refractive index of the PPKTP crystal determines the angular distribution of the generated SPDC light in the far-field through the temperature dependent phase-mismatch $\varphi(T)$. Fig. 2.3 (a), (b) and (c) show CCD images of the far-field intensity distribution of SPDC light at temperatures of 10°C, 30°C and 50°C generated in a 2 mm long PPKTP crystal. The pixel numbers were converted to far-field angles using the known size of the pixels of the CCD camera and focal length of the second lens f=25 mm that generates the far-field image. The down-converted photon emission is close to collinear phase matching ($\varphi \approx 0$) at the crystal temperature of 50°C, while at 10°C, the collected SPDC photons in the far-field form an open ring corresponding to a negative phase mismatch ($\varphi < 0$). In comparison to cw SPDC light, the intensity distribution of collinear SPDC has a shape that can be described by a Gaussian rather than the typical sinc shape of Eq. 2.1 for cw pump.

We recorded the intensity distribution of SPDC photons at 826.4 nm in the far-field from 2 mm, 5 mm and 10 mm long PPKTP crystals as a function of temperature between 10 and 50°C. In order to find the width (FWHM) and radius of the SPDC ring, each image is first converted to polar coordinates around its approximate center and then azimuthally averaged to obtain a radial distribution. We perform a numerical search that calculates the radial distribution as a function of center position to find the exact center that maximizes the peak intensity and minimizes the width. The radial intensity distribution obtained from the CCD images (a), (b) and (c) in Fig. 2.3 are shown in (d), (e) and (f), respectively. To determine the temperature dependent phase mismatch $\varphi(T)$, the radial intensity distribution for each crystal and all temperatures are fitted to Eq. (2.3) with ϕ, σ and an overall amplitude as fit parameters. Typical examples of the fit are shown by the solid lines in Fig. 2.3.

Fig. 2.4 shows the temperature dependence of the phase mismatch $\varphi(T)$,

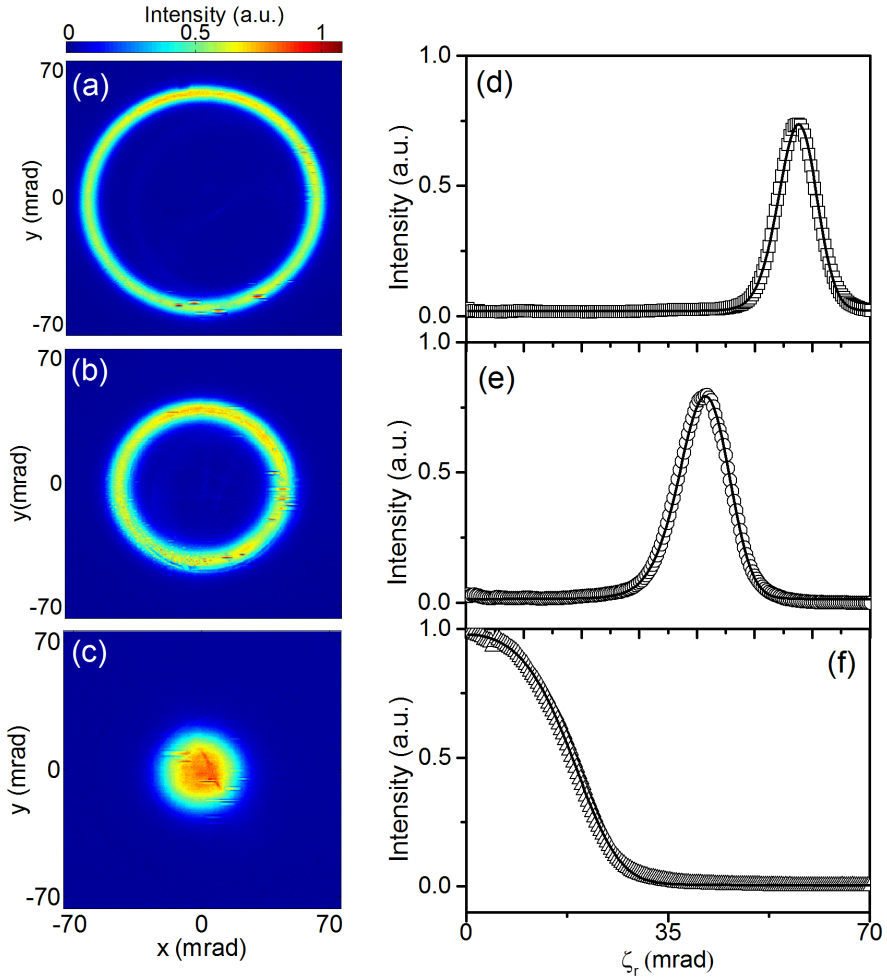

Figure 2.3: CCD images of the far-field distribution of SPDC light at 826.4 nm from a 2 mm PPKTP crystal pumped by 2 ps laser pulses at 413.2 nm and filtered by a 1 nm FWHM bandpass filter are shown for different temperatures of the crystal (a) T=10°C (b) T=30°C (c) T=50°C. (d), (e) and (f) correspond to radially integrated intensity of recorded far-field images as a function of far-field angle of the SPDC light. Solid lines are fits of Eq. (2.3) to the data (see text). Collinear phase matching is obtained close to a crystal temperature of 50°C.

which is related to the known temperature-dependent refractive index of PPKTP crystal [10, 15]. In order to describe the results in Fig. 2.4 and com-

pare them to literature, we introduce a Taylor expansion for the temperature dependent phase mismatch around a reference temperature of $T_r = 25^oC$ and find the coefficients α and β of the linear and quadratic temperature dependence.

$$\varphi(T) = \varphi(T_r) + \frac{1}{2}k_{2\omega}L[\alpha(T - T_r) + \beta(T - T_r)^2] \tag{2.4}$$

For non-collinear SPDC, the negative phase-mismatch provides a measure of the opening angle of the SPDC ring. Fig. 2.4 shows the phase-mismatch values extracted from the fit for the 2 mm (square), 5 mm (circles) and 10 mm (triangle) long PPKTP crystals as a function of temperature. The solid lines in Fig. 2.4 correspond to a best fit of Eq. 2.4 to the data.

L (mm)	α ($^\circ C^{-1}$) ($\times 10^{-6}$)	β ($^\circ C^{-2}$) ($\times 10^{-8}$)
2	26.1 ± 0.04	8.2 ± 0.3
5	27.4 ± 0.02	5.9 ± 0.2
10	26 ± 0.1	7.5 ± 0.6
5(cw)*	24.0 ± 0.02	4.8 ± 0.3

Table 2.1: The coefficients of the quadratic temperature dependence of the PPKTP crystal obtained from fitting the experimental results in Fig. 2.4 to Eq. 2.4. *The values of the coefficients obtained by cw pumping of a 5 mm crystal are shown as a reference [10].

The coefficients α and β of the temperature dependence of the PPKTP crystal obtained from the fit are shown in Table 2.1. In literature, an explicit expression for the temperature dependent refractive index of KTP crystal is given [15]. From this expression, the coefficients $\alpha = 23.56 \times 10^{-6}\ ^\circ C^{-1}$ and $\beta = 8.6 \times 10^{-8}\ ^\circ C^{-2}$ are found. Our values of α shown in Table 2.1 are comparable to the literature value, and the value found in experiments with a cw laser source using the exact same crystal [10]. The value of β is somewhat lower than the literature value, but is consistent with previous work for cw pumping using the same crystals as in this study [10]. As shown in Fig. 2.4, it is clear that the 5 mm PPKTP crystal has a slightly different collinear phase matching temperature compared to the 2 mm and 10 mm long crystals. The 2 and 10 mm crystals are grown by the manufacturer (Raicol crystals Ltd.) in a single batch, while the 5 mm crystal was produced by the same manufacturer

on a different date. Hence, we believe that the difference between crystals are due to small variations in crystal growth.

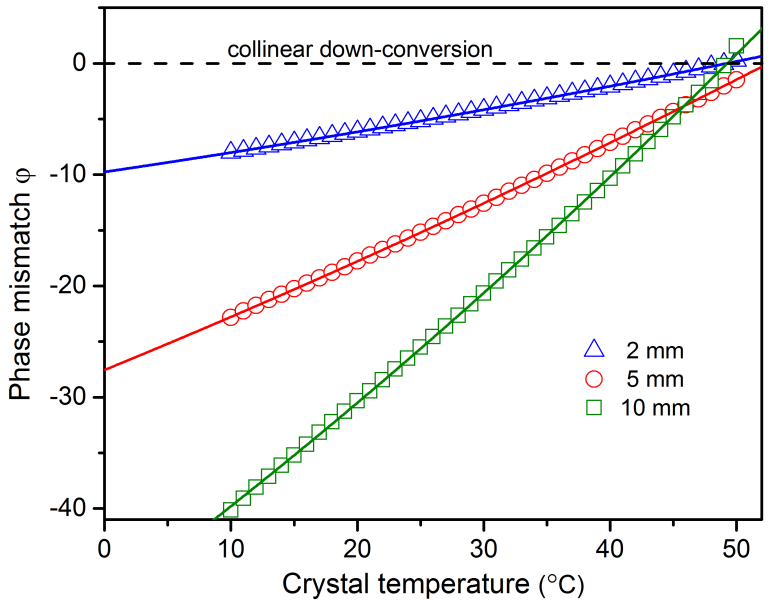

Figure 2.4: Phase-mismatch φ as a function of crystal temperature obtained from fitting the measured radial intensity distribution of SPDC ring pattern with the Eq. (2.3) for 2 mm (blue triangle), 5 mm (red circle) and 10 mm (green square) long PPKTP crystals. The solid lines show fits to the data (see text). The condition for collinear phase matching ($\varphi = 0$) is indicated by the horizontal dashed line.

Fig. 2.5 shows the experimentally determined temperature dependence of the angular width (FWHM) of the SPDC ring in pulsed down-conversion for three different crystal lengths. Data are shown for the 2 mm (blue triangles), 5 mm (red circles) and 10 mm (green squares) PPKTP crystals and are plotted as a function of phase-mismatch by using the temperature dependence of $\varphi(T)$ obtained from Fig. 2.4. The inset shows a false color plot of the radial intensity distribution as a function of phase-mismatch (bottom axis), crystal temperature (top axis) and angle for a 10 mm long PPKTP crystal. This clearly demonstrates the widening of the SPDC ring as the temperature is tuned toward the collinear phase-matching condition $\varphi = 0$. The sharp peak in the width as a function of phase-mismatch occurs at the point where the

intensity in the center equals half the intensity of the maximum and is a direct result of using the FWHM as a measure of the angular width.

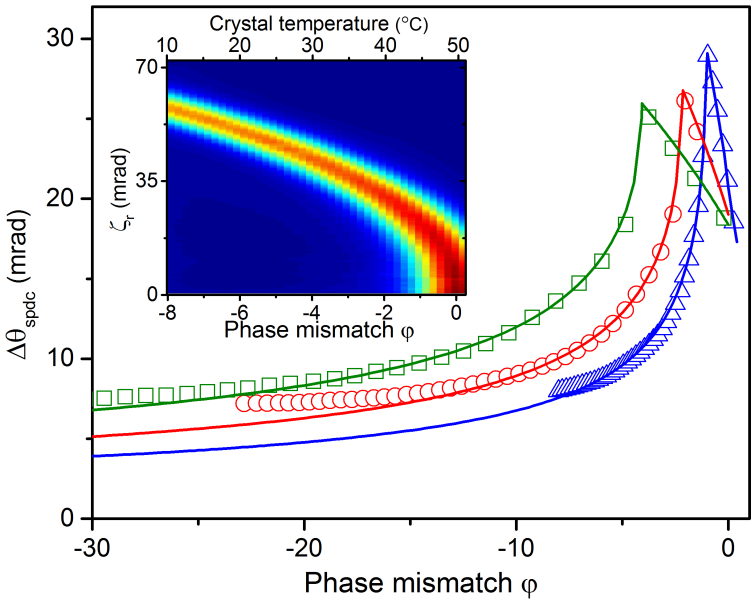

Figure 2.5: Angular width (FWHM) of SPDC ring patterns measured for various values of phase-matching of 2 mm (triangle), 5 mm (circle) and 10 mm (square) long PPKTP crystals obtained from fitting the radial intensity distribution to Eq. (2.3). The corresponding crystal temperature range is $10 - 50°$C for all crystals. The solid lines correspond to the angular width of the pulse predicted by Eq. (2.3) using spectral widths of $\sigma_{2mm} = 0.74$ rad/ps, $\sigma_{5mm} = 0.66$ rad/ps and $\sigma_{10mm} = 0.63$ rad/ps that best describes the data. The inset shows a false color plot of the radial intensity distributions as a function of crystal temperatures (top axis) and phase mismatch (bottom axis) for the 2 mm crystal.

For every crystal and each temperature we fit Eq. (2.3) to the radial intensity distribution and find a value for the spectral width σ that best describes the data. The solid lines in Fig. 2.5 correspond to the calculated angular width (FWHM) as obtained from Eq. (2.3) by setting a constant value for σ for each curve. We use a value σ = 0.74, 0.66 and 0.63 rad/ps for crystal lengths of 2, 5 and 10 mm, respectively. These values of σ are slightly larger than the transform-limited $\sigma = 0.59$ rad/ps for a 2 ps duration pulse as is commonly

observed for an actively mode-locked Ti:sapphire laser producing picosecond pulses [13] *. The fact that the value of σ depends on crystal length is not expected because σ is a property of the laser pulse. We remind the reader that Eq. (2.3) is an approximation for a plane-wave pump. The pump beam waist of 100 μm creates a spread in the pump beam transverse wavevector $\Delta\theta \sim \frac{\lambda_p}{w_p} \approx 4$ mrad. The diffraction limited angular width of the SPDC light is thus close to 8 mrad and explains the saturation of the ring width for large, negative phase mismatch.

Crystal	$n_g(2\omega) - n_g(\omega)$	$D\ (ps/mm)$	$d_{\text{eff}}\ (pm/V)$	$L_w d_{\text{eff}}^2\ (nm^3/V)$
PPKTP	0.456	1.5	9.8	125
PPLN	0.514	1.7	24.3	710
BBO	0.053	0.18	2.0	45
LBO	0.033	0.11	0.8	11
$LiIO_3$	0.154	0.51	3.4	45

Table 2.2: Group index mismatch $n_g(2\omega) - n_g(\omega)$, dispersion D and effective non-linearity d_{eff} for different crystals.

To create an efficient, pulsed source of SPDC light, non-linear crystals with a large second-order non-linearity are desirable. However, for crystals longer than the walk-off length $L_w = \tau/D$, the efficiency of the non-linear process of SPDC is reduced. To create bright sources of single photon pairs or sources that are capable of producing multiple pairs within a pulse it is important to consider the combined effect of the non-linear response and group velocity walk-off. For this purpose Table 2.2 summarizes the group index mismatch, dispersion D in ps/mm and the effective second-order non-linearity d_{eff} in pm/V. As can be seen from the table, the effective non-linearity of the crystals is strongly correlated with the dispersion D. This effect is similar to an empirical correlation between the linear and non-linear susceptibilities, known as Miller's rule [12, 16]. It is highly relevant here, because increase in performance due to a larger non-linearity is canceled by the effect of group velocity walk-off.

For a given spectral bandwidth of the bandpass filter used to collect the

*The manufacturer of our laser (Spectra-Physics) specifies a time-bandwidth product smaller than 1.7 times the Fourier limited time-bandwidth product

SPDC light the total number of photon pairs produced is proportional to the average laser power and the crystal length L. The intensity created by the non-linear process is thus proportional to $L\, d_{\text{eff}}^2$. This is valid for the common experimental situation of not too long crystal where the natural bandwidth of the SPDC light is much larger than the filter bandwidth. For pulsed lasers the useful length is limited to the group velocity walk-off length. Therefore we postulate that a good number to compare the pair production rate from different non-linear crystals is given by $L_w\, d_{\text{eff}}^2$

Table 2.2 compares this number for common non-linear crystals that could be used to create bright pair sources around 800 nm. The numbers in the table show that PPKTP and PPLN crystals are expected to outperform sources based on BBO or $LiIO_3$. It should be noted that the birefringent phase-matching required for BBO, LBO and $LiIO_3$ also introduces a spatial walk-off that depends on the waist of the pump beam. This spatial walk-off could shorten the length over which phase-matching is efficient and the number given in the table should be regarded as an upper limit for these crystals. For BBO the walk-off angle ρ is as large as 66 mrad, limiting the useful length for 100 μm waist of the pump beam in the experiment to only 1.5 mm. The walk-off angle in LBO is only 16 mrad, making the performance of LBO comparable to that of BBO when spatial walk-off becomes important. In contrast, periodically poled crystals such as PPKTP and PPLN do not suffer from spatial walk-off since the polarization of the pump and down-converted photons can be chosen to be identical. This greatly simplifies the design of the source. Given the large non-linearity of PPLN compared to PPKTP and a rather similar value of D, PPLN crystals would be preferred. This is especially true for processes that involve higher photon numbers as the yield of double pairs and triple pairs scales exponentially with the efficiency of the source. With current state-of-the-art poling technology for PPLN crystals sources that produce pairs at 980 nm would be feasible. Sources that operate around 800 nm, being the maximum detection efficiency of Si-based single photon counting detectors, seem to be within reach.

2.4 Conclusion

We have characterized and compared pulsed sources of frequency degenerate photons created by pulsed SPDC in a periodically poled KTP crystals of

different crystal lengths. For pulsed laser sources, group velocity dispersion becomes important and sets a limit to the length over which the SPDC process is efficient. For the 2 ps duration pulse in the experiment we estimate a group velocity walk-off length $L_w \approx 1.3$ mm. The experimentally observed radial intensity distributions as a function of temperature show a characteristic cone shaped emission pattern with an opening angle that increases with decreasing temperature. We find that the width (FWHM) of the open ring saturates at a value of $\sim$8 mrad for the lowest temperatures, independent of the crystal length (either 2, 5 or 10 mm in the experiment).

The radial intensity distribution is well described by a theoretical model that takes into account this group velocity walk-off. From fits of the model to the experimental data we obtain the co-linear phase-mismatch as a function of temperature. The temperature dependent phase-mismatch can be well approximated by a second order polynomial and is comparable to the temperature dependence for the same crystals pumped by a cw pump laser. Compared to literature values of the temperature-dependent refractive index of KTP crystal we find good agreement for the linear term and a small deviation in the quadratic term.

Bibliography

[1] Z. D. Walton, A. V. Sergienko, B. E. A. Saleh, and M. C. Teich, *Generation of polarization-entangled photon pairs with arbitrary joint spectrum*, Phys. Rev. A **70**, 052317 (2004).

[2] M. Fiorentino, G. Messin, C. E. Kuklewicz, F. N. C. Wong, and J. H. Shapiro, *Generation of ultrabright tunable polarization entanglement without spatial, spectral, or temporal constraints*, Phys. Rev. A **69**, 041801(R) (2004).

[3] Z. Y. Ou and L. Mandel, *Violation of Bell's inequality and classical probability in a two-photon correlation experiment*, Phys. Rev. Lett. **61**, 50 (1988).

[4] X. Li, L. Yang, X. Ma, L. Cui, Z. Y. Ou, and D. Yu, *All-fiber source of frequency-entangled photon pairs*, Phys. Rev. A **79**, 033817 (2009).

[5] S. Friberg, C. K. Hong, and L. Mandel, *Measurement of time delays in the parametric production of photon pairs*, Phys. Rev. Lett. **54**, 2011 (1985).

[6] H. D. Riedmatten, V. Scarani, I. Marcikic, A. Acn, W. Tittel, H. Zbinden, and N. Gisin, *Two independent photon pairs versus four-photon entangled states in parametric down conversion*, J. Mod. Opt. **51**, 1637 (2004).

[7] D. V. Strekalov, A. V. Sergienko, D. N. Klyshko, and Y. H. Shih, *Observation of two-photon ghost interference and diffraction*, Phys. Rev. Lett. **74**, 3600 (1995).

[8] C. K. Law and J. H. Eberly, *Analysis and interpretation of high transverse entanglement in optical parametric down conversion*, Phys. Rev. Lett. **92**, 127903 (2004).

[9] A. J. H. van der Torren, S. C. Yorulmaz, J. J. Renema, M. P. van Exter, and M. J. A. de Dood, *Spatially entangled four-photon states from a periodically poled potassium-titanyl-phosphate crystal*, Phys. Rev. A **85**, 043837 (2012).

[10] W. H. Peeters and M. P. van Exter, *Optical characterization of periodically-poled $KTiOPO_4$*, Optics Express **16**, 7344 (2008).

[11] T. E. Keller and M. H. Rubin, *Theory of two-photon entanglement for spontaneous parametric down-conversion driven by a narrow pump pulse*, Phys. Rev. A **56**, 1534 (1997).

[12] W. J. Alford and A. V. Smith, *Wavelength variation of the second-order nonlinear coefficients of $KNbO_3$, $KTiOPO_4$, $KTiOAsO_4$, $LiNbO_3$, $LiIO_3$, $\beta - BaB_2O_4$, HH_2PO_4 and LiB_3O_5 crystals: a test of Miller wavelength scaling*, J. Opt. Soc. Am. B **18**, 524 (2001).

[13] A. E. Siegman, *Lasers*, University Science Books, Sausalito, California, 1986.

[14] S. Wang, V. Pasiskevicius, F. Laurell, and H. Karlsson, *Ultraviolet generation by first-order frequency doubling in periodically poled $KTiOPO_4$*, Optics Letters **23**, 1883 (1998).

[15] S. Emanueli and A. Arie, *Temperature-dependent dispersion equations for $KTiOPO_4$ and $KTiOAsO_4$*, Applied Optics **42**, 33 (2003).

[16] R. C. Miller, *Optical second harmonic generation in piezo- electric crystals*, Appl. Phys. Lett. **5**, 17 (2003).